

# Infrared Spectra of Phenyl Nitrite and Phenoxy Radical–Nitric Oxide Complex in Solid Argon

Rongjing Yang, Xi Jin, Wenning Wang, Kangnian Fan, and Mingfei Zhou\*

Department of Chemistry & Laser Chemistry Institute, Shanghai Key Laboratory of Molecular Catalysts and Innovative Materials, Fudan University, Shanghai 200433, People's Republic of China

Received: January 7, 2005; In Final Form: March 25, 2005

Infrared spectra and frequency assignment of two isomers of nitrobenzene, namely the phenyl nitrite  $C_6H_5-ONO$  molecule and the phenoxy radical–nitric oxide complex  $C_6H_5O-NO$ , in solid argon are presented. The phenoxy radical–nitric oxide complex was produced through UV light irradiation of nitrobenzene in low-temperature solid argon matrix. The complex rearranged to the more stable phenyl nitrite molecule on sample annealing. The aforementioned species were identified on the basis of isotopic IR studies with  $C_6H_5^{15}NO_2$  and  $C_6D_5NO_2$ , as well as density functional theory calculations.

## Introduction

Nitrobenzene is a simple nitroaromatic compound. It serves as a prototypical molecule for combustion and decomposition of energetic materials and may also play an important role in atmospheric chemistry. The photodissociation of nitrobenzene has been the subject of various experimental and theoretical studies.<sup>1–11</sup> The photodissociation of nitrobenzene may follow many thermodynamically accessible channels and produce various products. An earlier emission study showed that nitrogen dioxide ( $NO_2$ ) and phenyl radical ( $C_6H_5$ ) are the dissociation products with a discharge lamp.<sup>1</sup> In another study, nitrosobenzene ( $C_6H_5NO$ ) was found after irradiation of a nitrobenzene sample.<sup>2</sup> Cyclopentadiene ( $C_5H_5$ ) has also been detected in the flash photolysis of nitrobenzene.<sup>3</sup> A later resonance enhanced multiphoton ionization study on nitrobenzene detected a number of  $C_nH_m$  ( $n = 1–6$ ,  $m = 0–5$ ) fragments as well as  $NO$ .<sup>4</sup> With the use of vacuum-ultraviolet photoionization mass spectrometry, three dissociation pathways leading to  $C_6H_5 + NO_2$ ,  $C_6H_5NO + O$ , and  $C_6H_5O + NO$  were observed in the photolysis of nitrobenzene at wavelengths between 220 and 280 nm.<sup>5,6</sup> The experimental observations suggest that many nitrobenzene molecules first rearranged to the phenyl nitrite ( $C_6H_5ONO$ ) intermediate and subsequently dissociated by breaking the C–ONO bond to release  $NO_2$ , the O–NO bond to produce  $NO$ , or the ON–O bond to form  $O$ .<sup>6</sup> Theoretical calculations supported the rearrangement pathway as the most likely dissociation channel for the production of  $NO$ .<sup>9,10</sup> The isomerization process from nitrobenzene to phenyl nitrite proceeded via a transition state with an energy barrier of 62.8 kcal/mol.<sup>12</sup> The calculations indicated that the phenyl nitrite intermediate may exist in two stable configurations of similar energy: a trans form and a cis form, so labeled depending on the N=O bond geometry with respect to the C–O bond. The trans structure was predicted to be only slightly (0.9 kcal/mol) lower in energy.<sup>11,12</sup> The free energy for trans to cis interconversion was calculated to be 0.9 kcal/mol (3.6 kJ/mol) at 298 K.<sup>11</sup>

Although the phenyl nitrite intermediate has been theoretically studied, it has not been experimentally characterized. The threshold energy for dissociation to  $C_6H_5O$  and  $NO$  was very

low; therefore, phenyl nitrite has very low stability. In the photodissociation experiments, the initially formed phenyl nitrite intermediate cannot be deactivated rapidly enough to stabilize the molecule with respect to dissociation.

Matrix isolation provides a powerful method for trapping reactive intermediates and free radicals. In a low-temperature solid matrix, the reaction can be very effectively quenched after the primary reaction or, at most, the earliest stages of the overall process. Transient reaction intermediates, which fragment readily in the gas phase, can usually be stabilized with removal of the internal thermal energy when they are trapped in the matrix environment.<sup>13</sup> Recent investigations in our laboratory have shown that transient reaction intermediates such as formylperoxy and vinylperoxy radicals can be effectively quenched and trapped in solid argon matrix for spectroscopic study.<sup>14,15</sup> In this paper, we report a combined matrix isolation infrared absorption spectroscopic and theoretical study of the phenyl nitrite and phenoxy radical–nitric oxide complex intermediates produced on the photodissociation of nitrobenzene in solid argon.

## Experimental and Theoretical Methods

The experimental setup for photodissociation and matrix isolation infrared absorption spectroscopic investigation has been described in detail previously.<sup>14,15</sup> Briefly, a gas stream containing  $C_6H_5NO_2/Ar$  was deposited onto a 4 K CsI window for 2 h at a rate of 3–5 mmol/h. The gas stream was subjected to broad-band UV–visible irradiation using a high-pressure mercury arc lamp with the globe removed (250–580 nm). Infrared spectra were recorded on a Bruker Equinox 55 spectrometer in the range of 400–4000  $cm^{-1}$  at 0.5  $cm^{-1}$  resolution using a DTGS detector. Matrix samples were annealed at different temperatures, selected samples were subjected to broad-band irradiation, and more spectra were taken. The  $C_6H_5NO_2/Ar$  mixture was prepared in a stainless steel vacuum line using a standard manometric technique.  $C_6H_5NO_2$  was cooled to 77 K using liquid  $N_2$  and evacuated to remove volatile impurities. Isotopically labeled samples  $C_6H_5^{15}NO_2$  (ISOTEC, 98%) and  $C_6D_5NO_2$  (ISOTEC, 99%) and selected mixtures were also prepared to elucidate the effects of isotopic substitution on the vibrational spectra of the reaction products.

\* Corresponding author. E-mail: mzhou@fudan.edu.cn.

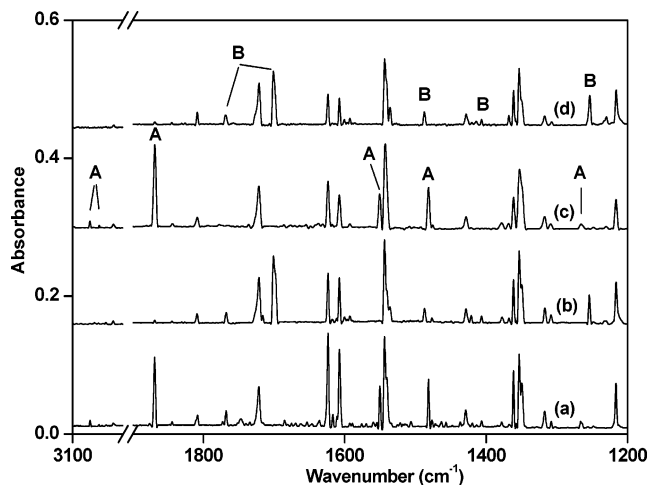


**Figure 1.** Infrared spectra in the 3100–3000 and 1900–1200  $\text{cm}^{-1}$  regions from deposition of 0.07%  $\text{C}_6\text{H}_5\text{NO}_2/\text{Ar}$  under broad-band irradiation at 4 K: (a) after 1 h of sample deposition, (b) after 30 K annealing, (c) after 30 min broad-band irradiation, and (d) after 35 K annealing.

Quantum chemical calculations were performed using the Gaussian 03 program.<sup>16</sup> Becke's three-parameter hybrid functional, with additional correlation corrections due to Lee, Yang, and Parr (B3LYP), was utilized.<sup>17,18</sup> The 6-311++G\*\* basis sets were used.<sup>19,20</sup> The geometries were fully optimized; the harmonic vibrational frequencies were calculated with analytic second derivatives, and zero point vibrational energies (ZPVE) were derived.

## Results and Discussion

**Infrared Spectra.** Experiments were performed in which the premixed  $\text{C}_6\text{H}_5\text{NO}_2/\text{Ar}$  gas mixture was deposited. The spectrum after deposition without broad-band irradiation shows only the nitrobenzene absorptions and trace water and  $\text{CO}_2$  and  $\text{CO}$  impurities. New product absorptions were observed when the deposited nitrobenzene sample was irradiated using a high-pressure mercury arc lamp. The same product absorptions were also produced in the experiments in which the gas mixture was irradiated in situ using the high-pressure mercury arc lamp during sample deposition. The spectra in the 3100–3000, 1900–1200, and 1100–425  $\text{cm}^{-1}$  regions from deposition of 0.07%  $\text{C}_6\text{H}_5\text{NO}_2/\text{Ar}$  under broad-band irradiation at 4 K are shown in Figures 1 and 2, respectively. As can be seen in the figures, a group of new bands at 3088.5, 3065.5, 3045.0, 1868.7, 1550.4, 1514.7, 1481.5, 1437.0, 1266.4, 1073.2, 897.2, 783.5, 633.4, 521.6, and 446.2  $\text{cm}^{-1}$ , which are labeled "A" in the figures (hereafter referred to as group A), were presented after 2 h of sample deposition (Figures 1a and 2a). The relative intensities of these new bands remained constant over a wide range of experiments and sample concentrations. In addition, very weak bands due to  $\text{C}_6\text{H}_5$  radical (706  $\text{cm}^{-1}$ ) were seen in some experiments.<sup>21</sup> When the matrix sample was annealed to 30 K, and then recooled to 4 K, all of the group A bands were completely absent (Figures 1b and 2b), and a group of new bands at 3067.8, 1701.6, 1600.3, 1595.0, 1486.3, 1233.8, 905.6, 764.7, 730.6, 688.6, 585.7, and 520.3  $\text{cm}^{-1}$ , which are labeled "B" in the figures (hereafter referred to as group B) were produced. Following another 30 min broad-band irradiation, the group B bands were destroyed, whereas the group A bands were recovered (Figures 1c and 2c). When the matrix sample was finally annealed to 35 K, and then recooled to 4 K, the group B bands were recovered and the group A bands were diminished

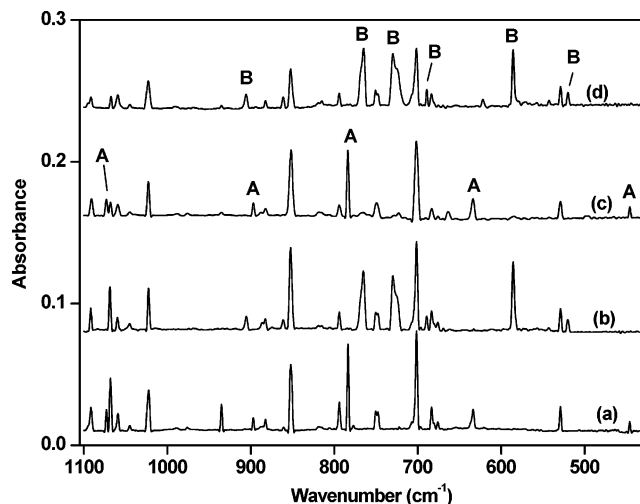


**Figure 2.** Infrared spectra in the 1100–425  $\text{cm}^{-1}$  region from deposition of 0.07%  $\text{C}_6\text{H}_5\text{NO}_2/\text{Ar}$  under broad-band irradiation at 4 K: (a) after 1 h of sample deposition, (b) after 30 K annealing, (c) after 30 min broad-band irradiation, and (d) after 35 K annealing.

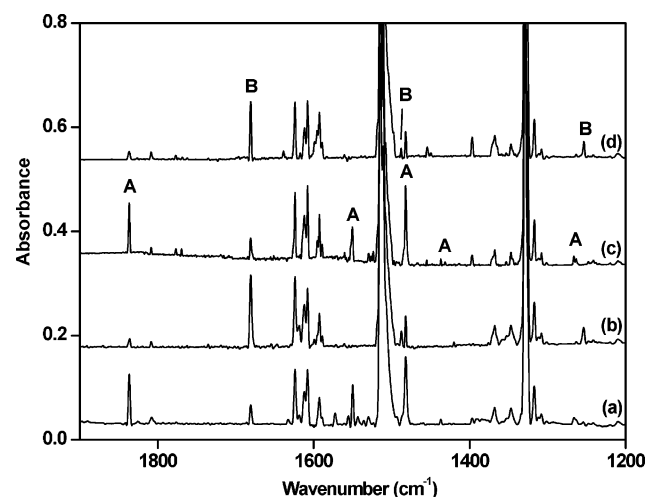


**Figure 3.** Infrared spectra in the 1900–1200  $\text{cm}^{-1}$  region from deposition of 0.07%  $\text{C}_6\text{H}_5^{15}\text{NO}_2/\text{Ar}$  under broad-band irradiation at 4 K: (a) after 2 h of sample deposition, (b) after 30 K annealing, (c) after 30 min broad-band irradiation, and (d) after 35 K annealing.

(Figures 1d and 2d). The bands of group B also maintained a constant intensity ratio with respect to one another from experiment to experiment, while their absolute intensities also varied directly with the intensities of the group A bands.

The experiments were repeated with the isotopically labeled  $\text{C}_6\text{H}_5^{15}\text{NO}_2$  and  $\text{C}_6\text{D}_5\text{NO}_2$  samples, and similar spectra were obtained. The spectra in selected regions with a 0.07%  $\text{C}_6\text{H}_5^{15}\text{NO}_2$  sample are illustrated in Figures 3 and 4, and the spectra using a 0.07%  $\text{C}_6\text{D}_5\text{NO}_2$  sample are shown in Figures 5 and 6, respectively. The new product absorptions and their isotopic counterparts are listed in Tables 1 and 2.

**$\text{C}_6\text{H}_5\text{O}-\text{NO}$ .** Broad-band UV–visible light irradiation (250  $\text{nm} < \lambda < 580 \text{ nm}$ ) of the deposited  $\text{C}_6\text{H}_5\text{NO}_2/\text{Ar}$  sample led to the observation of the group A bands, as listed in Table 1. These bands are assigned to different vibrational modes of the  $\text{C}_6\text{H}_5\text{O}-\text{NO}$  complex. The band assignments are straightforward, based on comparison to the previously reported phenoxyl radical ( $\text{C}_6\text{H}_5\text{O}$ ).<sup>22</sup> The most intense band at 1868.7  $\text{cm}^{-1}$  showed no shift when the  $\text{C}_6\text{D}_5\text{NO}_2$  sample was employed, but shifted to 1836.1  $\text{cm}^{-1}$  with the  $\text{C}_6\text{H}_5^{15}\text{NO}_2/\text{Ar}$  sample. The  $^{14}\text{N}/^{15}\text{N}$  isotopic ratio of 1.0178 is about the same as that of diatomic  $\text{NO}$  in solid argon (1.0179). The band position is only 3.1  $\text{cm}^{-1}$

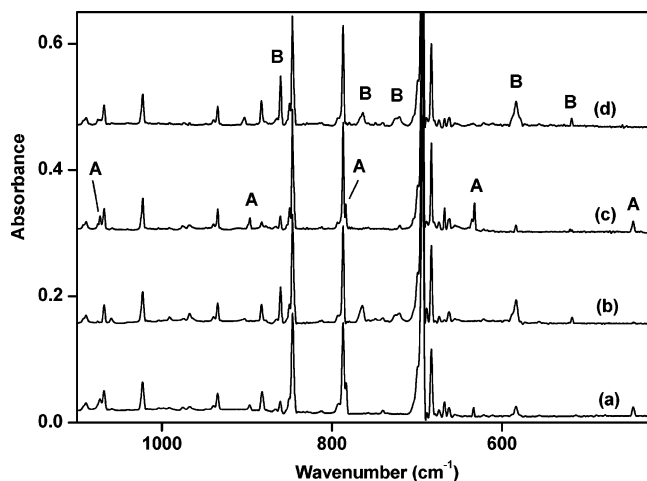


**Figure 4.** Infrared spectra in the 1100–425 cm<sup>-1</sup> region from deposition of 0.07% C<sub>6</sub>H<sub>5</sub><sup>15</sup>NO<sub>2</sub>/Ar under broad-band irradiation at 4 K: (a) after 2 h of sample deposition, (b) after 30 K annealing, (c) after 30 min broad-band irradiation, and (d) after 35 K annealing.

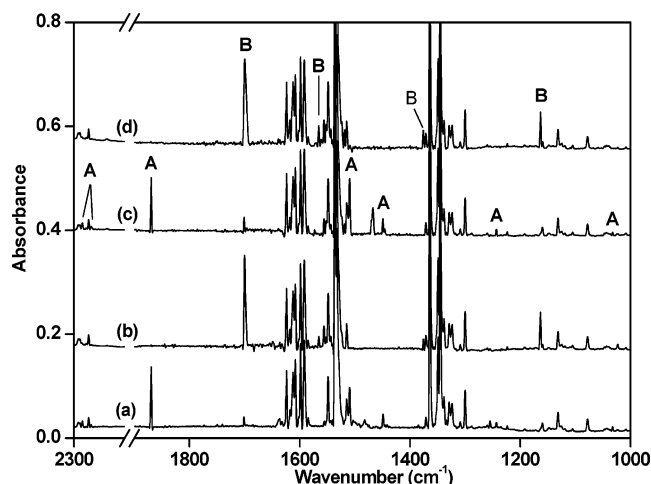


**Figure 5.** Infrared spectra in the 2300–2200 and 1900–1000 cm<sup>-1</sup> regions from deposition of 0.07% C<sub>6</sub>D<sub>5</sub>NO<sub>2</sub>/Ar under broad-band irradiation at 4 K: (a) after 2 h of sample deposition, (b) after 30 K annealing, (c) after 30 min broad-band irradiation, and (d) after 35 K annealing.

red-shifted from that of diatomic NO in solid argon. These observations indicate that the 1868.7 cm<sup>-1</sup> band is due to the N–O stretching vibration of a weakly perturbed NO complex. The other bands showed no isotopic shifts with the C<sub>6</sub>H<sub>5</sub><sup>15</sup>NO<sub>2</sub>/Ar sample, but exhibited shifts when the C<sub>6</sub>D<sub>5</sub>NO<sub>2</sub>/Ar sample was used. The band positions and isotopic frequency shifts are very similar to those of the phenoxyl radical in solid argon (most of the vibrational modes are within 2 cm<sup>-1</sup> differences).<sup>22</sup> The 3088.5, 3065.5, and 3045.0 cm<sup>-1</sup> bands are due to C–H stretching vibrations. The quite intense 1550.4 and 1481.5 cm<sup>-1</sup> bands exhibited small deuterium isotopic shifts (40.9 and 32.7 cm<sup>-1</sup>), and were assigned to the CC ring stretching and CO stretching modes. In the low-frequency region, the most intense bands were observed at 783.5 and 633.4 cm<sup>-1</sup>. The 783.5 cm<sup>-1</sup> band is due to the mixture of the chair deformation and CO/CH wagging mode, while the 633.4 cm<sup>-1</sup> band corresponds to the mixture of chair deformation and CH wagging of the C<sub>6</sub>H<sub>5</sub> ring. The assignments of the other less intense modes are listed in Table 1, and will not be discussed in detail here.

Density functional calculations were performed on the C<sub>6</sub>H<sub>5</sub>O–NO complex to support the experimental assignment. The optimized structure is shown in Figure 7, and the vibrational

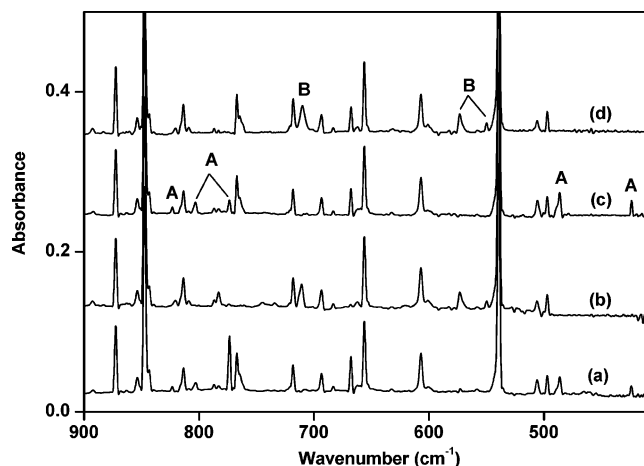


**Figure 6.** Infrared spectra in the 900–400 cm<sup>-1</sup> region from deposition of 0.07% C<sub>6</sub>D<sub>5</sub>NO<sub>2</sub>/Ar under broad-band irradiation at 4 K: (a) after 2 h of sample deposition, (b) after 30 K annealing, (c) after 30 min broad-band irradiation, and (d) after 35 K annealing.

**TABLE 1: Infrared Absorptions (cm<sup>-1</sup>) of the Phenoxyl Radical–Nitric Oxide Complex (C<sub>6</sub>H<sub>5</sub>O–NO) in Solid Argon**

C <sub>6</sub> H <sub>5</sub> NO <sub>2</sub>	C <sub>6</sub> H <sub>5</sub> <sup>15</sup> NO <sub>2</sub>	C <sub>6</sub> D <sub>5</sub> NO <sub>2</sub>	assignment
3088.5			C–H stretching
3065.5	3065.5	2284.2	C–H stretching
3045.0	3045.0	2266.8	C–H stretching
1868.7	1836.1	1868.7	N=O stretching
1550.4	1550.4	1509.5	CC ring stretching
1514.7			CC stretching + CH bending
1481.5	1481.5	1448.8	C=O stretching
1437.0	1437.0	1334.7	CC stretching + CH bending
1266.4	1266.4	1032.6	CC stretching + CH bending
1073.2	1073.2	823.2	CC stretching + CH bending
976.2			CCC bending
897.2	897.2	802.7	CH wagging + boat deforming
783.5	783.5	773.3	chair deformation + CO/CH wagging
633.4	633.4	486.1	chair deformation + CH wagging
521.6			CCC bending
446.2	446.2	423.3	CO bending

**TABLE 2: Infrared Absorptions (cm<sup>-1</sup>) of the Phenyl Nitrite (C<sub>6</sub>H<sub>5</sub>ONO) Molecule in Solid Argon**

C <sub>6</sub> H <sub>5</sub> NO <sub>2</sub>	C <sub>6</sub> H <sub>5</sub> <sup>15</sup> NO <sub>2</sub>	C <sub>6</sub> D <sub>5</sub> NO <sub>2</sub>	assignment
3067.8			C–H stretching
1701.6	1680.9	1701.6	N=O stretching
1600.3		1565.4	CC ring stretching
1595.0			CC stretching + CH bending
1486.3	1486.3	1375.9	CC stretching + CH bending
1233.8	1233.7	1162.9	C–O stretching
905.6	902.9	820.3	ring breathing + CCC bending
764.7	763.4		chair deformation + CO/CH wagging
730.6	726.8	710.1	ONO bending
688.6	688.6	549.5	chair deformation + CH wagging
585.7	583.8	573.6	CCC bending + ONO bending
520.3	518.5		CCC bending + ONO bending

frequencies and intensities are listed in Table 3. The B3LYP/6-311++G\*\* calculations indicate that the C<sub>6</sub>H<sub>5</sub>O–NO complex has a <sup>3</sup>A' ground state with a planar C<sub>s</sub> symmetry. The N atom of the NO subunit is coordinated to the oxygen atom of the C<sub>6</sub>H<sub>5</sub>O subunit with an N...O distance of 2.889 Å, indicating a very weak interaction between the two subunits. The bond length of the NO subunit was predicted to be 1.148 Å, elongated by 0.003 Å with respect to diatomic NO. The calculated N=O stretching vibrational frequency of the complex (1973.1 cm<sup>-1</sup>) is 6.6 cm<sup>-1</sup> red-shifted from that of free NO molecule (1979.7 cm<sup>-1</sup>) calculated at the same level. This value is slightly larger than the observed shift (3.1 cm<sup>-1</sup>). As listed in Table 3, the calculated vibrational frequencies of the C<sub>6</sub>H<sub>5</sub>O subunit are also in good agreement with the observed value. All the vibrational

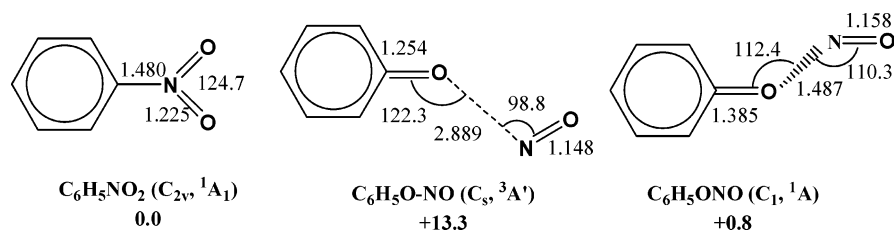


**Figure 7.** Optimized structures (bond lengths in angstroms and bond angles in degrees) and relative stabilities (kilocalories per mole) of the three  $C_6H_5NO_2$  isomers.

**TABLE 3: Comparison between Calculated and Observed Vibrational Frequencies ( $cm^{-1}$ ) and Intensities for the  $C_6H_5O-NO$  Complex**

calcd		exptl	
frequency	intensity <sup>a</sup>	frequency	intensity <sup>b</sup>
3201.5	1		
3197.5	5	3088.5	0.01
3188.7	12	3065.5	0.07
3173.5	9	3045.0	0.02
3166.7	1		
1973.1	75	1868.7	1.00
1585.3	43	1550.4	0.49
1544.3	4	1514.7	0.03
1484.2	45	1481.5	0.54
1441.7	5	1437.0	0.04
1417.7	2		
1339.7	6		
1227.8	7	1266.4	0.12
1167.4	0		
1165.1	2		
1090.6	9	1073.2	0.11
1008.5	0		
984.3	3	976.2	0.12
980.3	0		
979.0	1		
921.4	7	897.2	0.06
806.3	2		
798.2	0		
791.9	43	783.5	0.47
646.4	45	633.4	0.27
596.9	1		
532.2	3	521.6	0.04
475.7	1		
449.6	6	446.2	0.06
377.2	0		
186.5	3		
117.8	1		
55.9	2		
28.1	2		
20.9	1		
16.9	1		

<sup>a</sup> In  $km/mol$ . <sup>b</sup> Integrated intensity normalized to the most intense absorption.

modes that were predicted to have IR intensities higher than 3  $km/mol$  in our spectral range were experimentally observed with the integrated IR intensities, in reasonable agreement with the calculated relative intensity ratios except the  $1339.7\text{ cm}^{-1}$  mode. The calculated  $1339.7\text{ cm}^{-1}$  band is due to a mixed mode of CC stretching and CH bending. This mode was predicted to have 6  $km/mol$  harmonic IR intensity. The same vibrational mode of the  $C_6H_5O$  radical was observed at  $1318\text{ cm}^{-1}$  in solid argon.<sup>22</sup> This mode of the  $C_6H_5O-NO$  complex is most likely overlapped by the strong absorption of  $C_6H_5NO_2$  at  $1317.5\text{ cm}^{-1}$ . The agreement between theory and experiment for some of the frequencies listed in Table 3 is not very good. We note that the calculated frequencies listed in Table 3 are unscaled harmonic frequencies. The matrix environment may also have different effects on different vibrational modes. The calculated isotopic frequency shifts are in good agreement with the observed values and provide additional support for the complex assignment.

$C_6H_5ONO$ . The bands of group B appeared upon sample annealing at the expense of the  $C_6H_5O-NO$  complex (group A). These two groups of product absorptions can be interconverted via broad-band irradiation and sample annealing, which suggests that the bands of group B are due to a more stable structural isomer of the  $C_6H_5O-NO$  complex. The bands of group B, as listed in Table 2, are assigned to different vibrational modes of the phenyl nitrite  $C_6H_5ONO$  molecule based on isotopic substitutions and comparison to the theoretical calculations.

The phenyl nitrite  $C_6H_5ONO$  molecule has been suggested to be a key intermediate in the photodissociation of nitrobenzene, and has been the subject of several previous theoretical calculations.<sup>9-12</sup> The phenyl nitrite molecule may exist in two stable configurations of similar energy: a trans form and a cis form, so labeled depending on the C-O bond geometry with respect to the N=O bond. Previous theoretical calculations indicated that both structures are local minima on the potential energy surface and are slightly less stable than the nitrobenzene isomer.<sup>11,12</sup> The trans structure is slightly more stable than the cis structure. The cis structure was predicted to possess a  $C_s$  symmetry with the mirror plane containing the ONO group, whereas the trans structure has a nonplanar  $C_1$  symmetry. In agreement with previous calculations, all the vibrational frequencies for both structures are real at the B3LYP/6-31G\* level of theory.<sup>11</sup> However, the cis structure was calculated to exhibit an imaginary frequency at the higher B3LYP/6-311++G\*\* level of theory, which indicates that the cis structure is a transition state. The optimized trans structure is shown in Figure 7, and the vibrational frequencies and intensities are listed in Table 4.

The strongest band of  $C_6H_5ONO$  was observed at  $1701.6\text{ cm}^{-1}$ . This band is due to the N=O stretching mode. It showed no shift with  $C_6D_5NO_2$ , but shifted to  $1680.9\text{ cm}^{-1}$  with  $C_6H_5^{15}NO_2$ . This mode for trans  $C_6H_5ONO$  was calculated at  $1800.9\text{ cm}^{-1}$  with a  $^{14}N/^{15}N$  ratio of 1.0123, the same as the experimental value. The weak  $1600.3\text{ cm}^{-1}$  band is due to the CC ring stretching vibration, which was predicted at  $1631.9\text{ cm}^{-1}$ . The observed shift with  $C_6D_5NO_2$  is  $34.9\text{ cm}^{-1}$ , while the calculation gave a value of  $34.0\text{ cm}^{-1}$ . The very weak band at  $1595.0\text{ cm}^{-1}$  is most likely a mixed mode of CC stretching and CH bending. This mode was computed to absorb at  $1628.4\text{ cm}^{-1}$ . The  $1486.3\text{ cm}^{-1}$  band, which showed no shift with  $C_6H_5^{15}NO_2$  and  $110.4\text{ cm}^{-1}$  shift with  $C_6D_5NO_2$ , is attributed to a mixed CC stretching and CH bending mode. This mode was predicted at  $1514.8\text{ cm}^{-1}$  with a  $120.2\text{ cm}^{-1}$  deuterium shift. The  $1233.8\text{ cm}^{-1}$  band is assigned to the C-O stretching mode calculated at  $1227.1\text{ cm}^{-1}$ . The  $764.7\text{ cm}^{-1}$  band is the third strongest band, and is assigned to the mixture of chair deformation and CO/CH wagging mode, which was predicted at  $780.7\text{ cm}^{-1}$ . The  $730.6\text{ cm}^{-1}$  band is the second strongest band and is attributed to the ONO bending mode, which was computed at  $731.8\text{ cm}^{-1}$ . The  $688.6\text{ cm}^{-1}$  band showed no shift with  $C_6H_5^{15}NO_2$ , and  $139.1\text{ cm}^{-1}$  shift with  $C_6D_5NO_2$ . This band

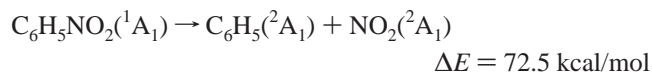
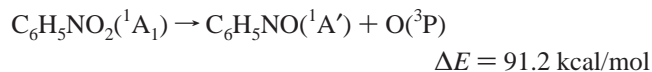
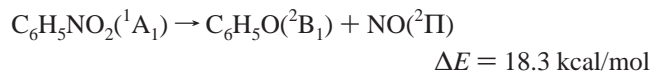
**TABLE 4: Comparison between Calculated and Observed Vibrational Frequencies (cm<sup>-1</sup>) and Intensities for the C<sub>6</sub>H<sub>5</sub>ONO Molecule**

calcd		expt	
frequency	intensity <sup>a</sup>	frequency	intensity <sup>b</sup>
3200.4	1		
3197.5	7		
3189.2	17	3067.8	0.02
3177.7	8		
3168.6	0		
1800.9	505	1701.6	1.00
1631.9	27	1600.3	0.04
1628.4	13	1595.0	0.02
1514.8	63	1486.3	0.11
1484.4	2		
1347.1	0		
1328.2	1		
1227.1	74	1233.8	0.21
1185.9	8		
1180.2	4		
1097.6	10		
1042.9	5		
1016.7	0		
980.4	0		
972.0	10		
929.3	48	905.6	0.07
900.1	9		
838.7	1		
780.7	151	764.7	0.46
731.8	174	730.6	0.55
689.0	44	688.6	0.05
632.1	8		
584.9	197	585.7	0.33
530.2	35	520.3	0.05
459.6	8		
419.3	0		
348.9	68		
289.1	4		
157.0	1		
127.8	1		
62.8	1		

<sup>a</sup> In km/mol. <sup>b</sup> Integrated intensity normalized to the most intense absorption.

is assigned to the mixed mode of chair deformation and CH wagging. This mode was predicted at 689.0 cm<sup>-1</sup> with 136.8 cm<sup>-1</sup> deuterium shift. The 585.7 cm<sup>-1</sup> band is also quite intense (about 30% intensity of the strongest N=O stretching mode). This band exhibited very small nitrogen-15 (1.9 cm<sup>-1</sup>) and deuterium (12.1 cm<sup>-1</sup>) isotopic shifts, and is assigned to a mode of CCC bending and ONO bending. This mode was computed at 584.9 cm<sup>-1</sup>, with 1.8 cm<sup>-1</sup> nitrogen-15 and 9.5 cm<sup>-1</sup> deuterium isotopic shifts. The much weaker band at 520.3 cm<sup>-1</sup> is due to a mode similar to that for the 585.7 cm<sup>-1</sup> band.

**Reaction Mechanisms.** The photodissociation of nitrobenzene has been well studied in the gas phase. Several dissociation channels were observed.<sup>1–5</sup> The required heats of formation for different channels were predicted as listed below:<sup>23–26</sup>



Previous studies indicated that the photodissociation process to form C<sub>6</sub>H<sub>5</sub>O + NO proceeded via the phenyl nitrite

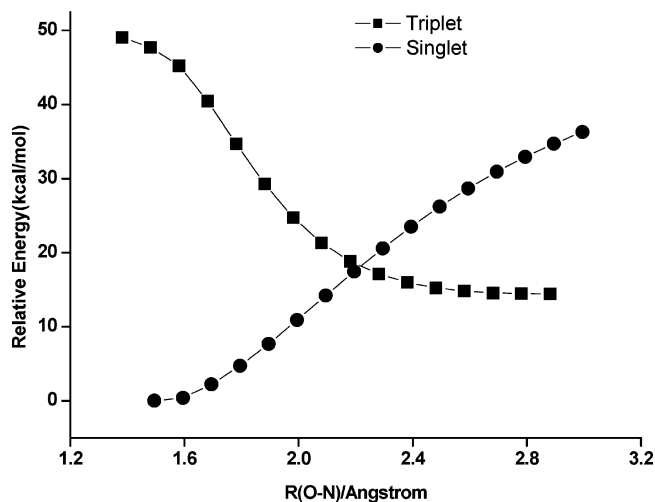


**Figure 8.** Potential energy curves along the O–N bond of triplet C<sub>6</sub>H<sub>5</sub>O–NO complex and singlet C<sub>6</sub>H<sub>5</sub>ONO molecule evaluated at the B3LYP/6-311G\*\* level of theory.

intermediate. The isomerization reaction from nitrobenzene to phenyl nitrite is almost thermal neutral (nitrobenzene is predicted to be about 0.8 kcal/mol lower in energy than phenyl nitrite), but requires an energy barrier of 62.8 kcal/mol. In the present experiments, broad-band UV/visible light from a high-pressure mercury arc lamp (250–580 nm) was employed for irradiation, but filtered experiments indicated that only the light in the wavelength range of 250–300 nm is responsible for nitrobenzene dissociation. The photon energy in this wavelength range is sufficient to overcome the energy barrier for isomerization reaction from nitrobenzene to phenyl nitrite. The initially formed phenyl nitrite is highly excited, and cannot be stabilized even in the 4 K solid argon matrix. It rapidly dissociated to the phenoxy radical and nitric oxide as observed in the gas phase. The in situ formed C<sub>6</sub>H<sub>5</sub>O and NO fragments cannot escape the matrix “cage”, and recombine to form the C<sub>6</sub>H<sub>5</sub>O–NO complex due to the matrix cage effect. At present experimental conditions, the formation of phenoxy radical and nitric oxide is the dominant reaction channel for nitrobenzene dissociation. No C<sub>6</sub>H<sub>5</sub>NO and NO<sub>2</sub> absorptions were observed in the experiments. Upon sample annealing, the C<sub>6</sub>H<sub>5</sub>O–NO complex absorptions disappeared, while the C<sub>6</sub>H<sub>5</sub>ONO absorptions appeared. This implies that the complex rearranged to the more stable C<sub>6</sub>H<sub>5</sub>ONO isomer. Our B3LYP/6-311++G\*\* calculations predicted that phenyl nitrite is about 12.5 kcal/mol lower in energy than the C<sub>6</sub>H<sub>5</sub>O–NO complex. The rearrangement process proceeds on annealing the matrix sample to around 25 K, which indicates that this process requires very low activation energy. Since the C<sub>6</sub>H<sub>5</sub>O–NO complex has a triplet ground state, while the C<sub>6</sub>H<sub>5</sub>ONO molecule has a singlet ground state, the rearrangement process requires spin crossing. We calculated the minimized energy curves along the O–N bond on the potential energy surfaces of singlet C<sub>6</sub>H<sub>5</sub>ONO molecule and triplet C<sub>6</sub>H<sub>5</sub>O–NO complex at the B3LYP/6-311G\*\* level of theory. The curves are depicted in Figure 8. The energy barrier for the rearrangement process is estimated from the energy difference between the stable C<sub>6</sub>H<sub>5</sub>O–NO complex and the crossing point of the two energy curves, with a value of 3.7 kcal/mol. The association reaction between C<sub>6</sub>H<sub>5</sub>O radical and NO was previously studied with the cavity-ring-down method in the gas phase in the temperature range 297–373 K.<sup>27</sup> The results showed that the association reaction has a negative activation energy of 0.8 kcal/mol. Both our experimental results and theoretical calculations clearly indicate that nonzero activa-

tion energy is required for the reaction from  $C_6H_5O-NO$  to  $C_6H_5ONO$ . We also considered two other  $C_6H_5NO_2$  isomers, which could be formed directly by association reaction between NO and phenoxy radical, when the NO radical attaches  $C_6H_5O$  to the ortho carbon and para carbon, respectively. These two isomers were predicted to be 17.2 and 15.5 kcal/mol higher in energy than  $C_6H_5NO_2$ , and no evidence was found for the formation of these two isomers in the present experiments.

### Conclusions

The products from UV photon induced dissociation or isomerization of nitrobenzene in solid argon have been studied using infrared absorption spectroscopy as well as density functional calculations. The weakly bonded phenoxy radical–nitric oxide complex ( $C_6H_5O-NO$ ) was produced upon UV irradiation of nitrobenzene. The complex rearranged to the more stable phenyl nitrite molecule upon sample annealing. The  $C_6H_5O-NO$  complex was predicted to have a triplet ground state with a planar  $C_s$  symmetry, while the phenyl nitrite molecule was predicted to have a nonplanar structure with the C–O bond in a trans position relative to the N–O bond. The  $C_6H_5O-NO$  complex and the  $C_6H_5ONO$  molecule can be interconverted in solid argon matrix via UV irradiation or sample annealing. Fifteen vibrational modes for the  $C_6H_5O-NO$  complex and 12 modes for the  $C_6H_5ONO$  molecule were identified and assigned.

**Acknowledgment.** We greatly acknowledge financial support from the NNSFC (Grant 20473023) and the Committee of Science and Technology of Shanghai (04JC14016).

### References and Notes

- Schuler, V. H.; Woeldike, A. *Phys. Z.* **1944**, *45*, 171.
- Hastings, S. H.; Matsen, F. A. *J. Am. Chem. Soc.* **1948**, *70*, 3514.
- Poter, G.; Ward, B. *Proc. R. Soc. London, Ser. A* **1968**, *303*, 139.
- Marshall, A.; Clark, A.; Jennings, R.; Ledingham, K. W. D.; Singhal, R. P. *Int. J. Mass Spectrom. Ion Processes* **1992**, *112*, 273.
- Galloway, D. B.; Bartz, J. A.; Huey, L. G.; Crim, F. F. *J. Chem. Phys.* **1993**, *98*, 2107.
- Douglas, B. G.; Glenewinkel-Meyer, T.; Bartz, J. A.; Huey, L. G.; Crim, F. F. *J. Chem. Phys.* **1994**, *100*, 1946.
- Kosmidis, C.; Ledingham, K. W. D.; Kilic, H. S.; McCanny, T.; Singhal, R. P.; Langley, A. J.; Shaikh, W. *J. Phys. Chem. A* **1997**, *101*, 2264.
- Berho, F.; Caralp, F.; Rayez, M. T.; Lesclaux, R.; Ratajczak, E. *J. Phys. Chem. A* **1998**, *102*, 1.
- Glenewinkel-Meyer, T.; Crim, F. F. *J. Mol. Struct. (THEOCHEM)* **1995**, *337*, 209.
- Castle, K. J.; Abbott, J.; Peng, X. Z.; Kong, W. *J. Chem. Phys.* **2000**, *113*, 1415.
- Polasek, M.; Turecek, F.; Gerbaux, P.; Flammang, R. *J. Phys. Chem. A* **2001**, *105*, 995.
- Li, Y. M.; Sun, J. L.; Yin, H. M.; Han, K. L.; He, G. Z. *J. Chem. Phys.* **2003**, *118*, 6244.
- Jacox, M. E. *Chemistry and Physics of Matrix-Isolated Species*; Andrews, L., Moskovits, M., Eds., North-Holland: Amsterdam, 1989.
- Yang, R. J.; Yu, L.; Zeng, A. H.; Zhou, M. F. *J. Phys. Chem. A* **2004**, *108*, 4228.
- Yang, R. J.; Yu, L.; Jin, X.; Zhou, M. F.; Carpenter, B. K. *J. Chem. Phys.* **2005**, *122*, 014511.
- Frisch, M. J.; Trucks, G. W.; Schlegel, H. B.; Scuseria, G. E.; Robb, M. A.; Cheeseman, J. R.; Montgomery, J. A., Jr.; Vreven, T.; Kudin, K. N.; Burant, J. C.; Millam, J. M.; Iyengar, S. S.; Tomasi, J.; Barone, V.; Mennucci, B.; Cossi, M.; Scalmani, G.; Rega, N.; Petersson, G. A.; Nakatsuji, H.; Hada, M.; Ehara, M.; Toyota, K.; Fukuda, R.; Hasegawa, J.; Ishida, M.; Nakajima, T.; Honda, Y.; Kitao, O.; Nakai, H.; Klene, M.; Li, X.; Knox, J. E.; Hratchian, H. P.; Cross, J. B.; Adamo, C.; Jaramillo, J.; Gomperts, R.; Stratmann, R. E.; Yazyev, O.; Austin, A. J.; Cammi, R.; Pomelli, C.; Ochterski, J. W.; Ayala, P. Y.; Morokuma, K.; Voth, G. A.; Salvador, P.; Dannenberg, J. J.; Zakrzewski, V. G.; Dapprich, S.; Daniels, A. D.; Strain, M. C.; Farkas, O.; Malick, D. K.; Rabuck, A. D.; Raghavachari, K.; Foresman, J. B.; Ortiz, J. V.; Cui, Q.; Baboul, A. G.; Clifford, S.; Cioslowski, J.; Stefanov, B. B.; Liu, G.; Liashenko, A.; Piskorz, P.; Komaromi, I.; Martin, R. L.; Fox, D. J.; Keith, T.; Al-Laham, M. A.; Peng, C. Y.; Nanayakkara, A.; Challacombe, M.; Gill, P. M. W.; Johnson, B.; Chen, W.; Wong, M. W.; Gonzalez, C.; Pople, J. A. *Gaussian 03*, Revision B.05; Gaussian, Inc.: Pittsburgh, PA, 2003.
- Becke, A. D. *J. Chem. Phys.* **1993**, *98*, 5648.
- Lee, C.; Yang, E.; Parr, R. G. *Phys. Rev. B* **1988**, *37*, 785.
- McLean, A. D.; Chandler, G. S. *J. Chem. Phys.* **1980**, *72*, 5639.
- Krishnan, R.; Binkley, J. S.; Seeger, R.; Pople, J. A. *J. Chem. Phys.* **1980**, *72*, 650.
- Friderichsen, A. V.; Radziszewski, J. G.; Nimlos, M. R.; Winter, P. R.; Dayton, D. C.; David, D. E.; Ellison, G. B. *J. Am. Chem. Soc.* **2001**, *123*, 1977.
- Spanget-Larsen, J.; Gil, M.; Gorski, A.; Blake, D. M.; Waluk, J.; Radziszewski, J. G. *J. Am. Chem. Soc.* **2001**, *123*, 11253.
- Handbook of Bond Dissociation Energies in Organic Compounds*; Luo, Y. R., Ed.; CRC Press: Boca Raton, FL, 2002.
- Chase, M. W., Jr. *J. Phys. Chem. Ref. Data, Monogr.* **1998**, No. 9.
- Choo, K. Y.; Golden, D. M.; Benson, S. W. *Int. J. Chem. Kinet.* **1975**, *7*, 713.
- Pedley, J. B.; Naylor, R. D.; Kirby, S. P. *Thermochemical Data of Organic Compounds*; Chapman & Hall: New York, 1986; pp 1–792.
- Yu, T.; Mebel, A. M.; Lin, M. C. *J. Phys. Org. Chem.* **1995**, *8*, 47.